Cancer Imaging (2012) **12**, 506–515
DOI: 10.1102/1470-7330.2012.0039

CI

e-med
www.e-med.org.uk

REVIEW

Imaging of anterior mediastinal tumours

Ching Ching Ong, Lynette L.S. Teo

Department of Diagnostic Imaging, National University Hospital, 1E Kent Ridge Road, Singapore

Corresponding address: Dr. Lynette L.S. Teo, Department of Diagnostic Imaging, National University Hospital, 1E Kent Ridge Road, Tower block, Level 12, Singapore 119074.
Email: lynette_ls_teo@nuhs.edu.sg

Date accepted for publication 7 August 2012

Abstract

Anterior mediastinal tumours include primary and secondary tumours. Patients may be asymptomatic or present with symptoms related to local tumour invasion or systemic symptoms due to release of hormones/cytokines or antibodies. The most common symptoms at presentation include chest pain, dyspnoea, cough, fever and chills. Despite rapid developments in imaging techniques, accurate staging of anterior mediastinal tumours remains a diagnostic quandary. Multimodality imaging plays an important role in determining surgical resectability and/or impact on subsequent management. This article briefly discusses the epidemiology and incidence of anterior mediastinal tumours and describes the role of imaging in tumour characterization and staging in detail. We focus on the more commonly encountered anterior mediastinal tumours.

Keywords: *Anterior mediastinal tumours; imaging; staging; computed tomography; magnetic resonance imaging.*

Introduction

Anterior mediastinal tumours comprise a diverse group of benign and malignant primary and secondary neoplasms (Table 1). Imaging would aid clinical management if these neoplasms could be differentiated and accurately staged, as treatment and prognosis vary greatly.

Epidemiology

Of all primary mediastinal tumours, 54% occur in the anterior mediastinum, 20% in the middle mediastinum and 26% in the posterior mediastinum[1]. The most common primary anterior mediastinal tumours are thymomas (30%), lymphomas (20%), germ cell tumours (18%) and carcinomas (13%)[1]. Secondary tumours are more common than primary tumours and include metastatic nodes from primary tumours of the lung, oesophagus and testis[2,3].

Clinical presentation

Mediastinal tumours may present at any age, although they occur predominantly in the third to fifth decades[2]. The presence of symptoms is a predictor of malignancy. Davis et al.[1] found that 85% of patients with malignant mediastinal tumours were symptomatic versus 46% of patients with benign tumours. Also, 83% of mediastinal masses in asymptomatic patients were benign, whereas 57% in symptomatic patients were malignant[1]. There may be localizing symptoms (from tumour compression or direct invasion of adjacent structures) or systemic symptoms (paraneoplastic syndromes from release of hormones/cytokines/antibodies). The most common symptoms are chest pain, cough, dyspnea and fever and chills.

Imaging

Radiographs show an anterior mediastinal mass where the hilum overlay sign and silhouette sign with the cardiac border are present, together with preservation of the posterior mediastinal lines (Fig. 1a)[4,5]. Masses in the superior-anterior mediastinum with tracheal deviation are mostly of thyroid origin. Masses in the prevascular space can obliterate the anterior junction line.

Ultrasonography allows differentiation of solid from cystic masses. Due to limited acoustic windows,

This paper is available online at http://www.cancerimaging.org. In the event of a change in the URL address, please use the DOI provided to locate the paper.

Table 1 **Classification of anterior mediastinal tumours (adapted from Reference 3)**

Benign	Malignant
Masses of thymic origin	
Thymic hyperplasia	
Thymolipoma	
Thymic cyst	Thymic cyst
– congenital	– acquired (neoplasm)
– acquired(inflammation)	
Thymoma (benign)	Thymoma (invasive)
	Thymic carcinoma
Germ cell tumours	
Mature teratoma	Immature teratoma
	Teratoma with malignant transformation
	Seminoma
	Non-seminomatous tumours
	– endodermal sinus tumours
	– choriocarcinomas
	– embryonal carcinoma
	Mixed germ cell tumours
Lymph node masses	
Inflammation	Metastases
Granulomatosis	Systemic lymphoma
Sarcoidosis	Primary mediastinal lymphoma
	– Hodgkin lymphoma
	– Non-Hodgkin lymphoma (diffuse large B-cell lymphoma and T-cell lymphoblastic lymphoma)
Thyroid masses	
Goitre	
Thyroid adenoma	Thyroid carcinoma
Parathyroid masses	
Parathyroid hyperplasia	Parathyroid carcinoma
Parathyroid adenoma	
Mesenchymal masses originating from adipose tissue	
Lipomatosis	Liposarcoma
Lipoma	
Mesenchymal masses originating from lymphatic vessels	
Lymphangioma	Lymphangiosarcoma
	Lymphangiopericytoma
Mesenchymal masses originating from blood vessels	
Haemangioma	Malignant haemangiopericytoma
Haemangioendothelioma	Angiosarcoma
Benign haemangiopericytoma	
Congenital cysts	
Pericardial mesothelial cysts	
Bronchogenic cyst	

it is used in selected cases, especially in paediatric patients and in assessing thyroid and parathyroid diseases.

Computed tomography (CT) allows accurate localization and determination of tumour extent. It characterizes the nature of the mass and identifies fat and calcification.

Expiratory dynamic CT (EDCT) can help evaluate tumour invasion into the chest wall or mediastinum as free movement of tumour is direct evidence of the absence of attachment between visceral and parietal pleura[6]. However, difficulty exists in distinguishing between invasive tumour and benign adhesions. Furthermore, assessment of tumour movement on axial CT images is difficult for tumours near the lung apex or diaphragm[6]. There is increase in radiation dose from additional scanning during expiration.

Magnetic resonance imaging (MRI) is increasingly utilized due to faster breathhold and cardiac-gated sequences. Advantages include excellent soft tissue contrast, multiplanar capabilities and lack of ionizing radiation. However, MRI may not detect calcification and requires a longer scan time. Cardiac-gated cine steady-state free precession (SSFP) and T1-weighted (T1W) spin echo sequences are helpful in evaluating tumour invasion into the mediastinum and chest wall[7]. Intervening fat planes are better visualized on MRI (Fig. 2c,d)[7]. Some studies report that respiratory dynamic (RD) MRI is useful for assessing tumour invasion[8,9]. This technique is superior to EDCT in evaluating tumours near the lung apex as such tumour movement is more easily detected on sagittal or coronal images[8].

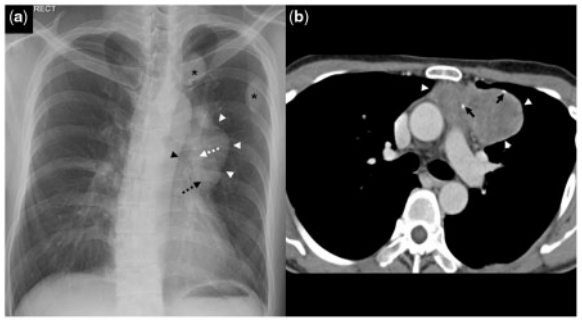

Figure 1 **A 35-year-old man with thymoma (WHO B3) and dropped pleural metastases. (a) Frontal chest radiograph shows a mass (white arrowheads) projected over the left hilum. The hilum overlay sign (dotted white arrow) and silhouette sign with the left heart border (dotted black arrow) are present. There is also preservation of the descending thoracic aorta border (black arrowhead). This is in keeping with an anterior mediastinal mass. A few pleural-based nodules (black asterisks) are seen in the left upper zone. (b) Contrast-enhanced axial CT image shows a soft tissue mass (white arrowheads) with specks of calcification (black arrows) in the left anterior mediastinum.**

Fluorodeoxyglucose (FDG)-positron emission tomography (PET) aids in the diagnosis and evaluation of treatment response, especially in lymphomas and germ cell tumours[4].

Surgical resectability

Absolute contraindications to resection include invasion of the myocardium, great vessels or trachea[10]. The most commonly invaded structure is the pericardium; followed by the pleura, lungs, phrenic nerve and superior vena cava (SVC)[10]. Current CT criteria used to determine mediastinal invasion are the extent of contact between the mass and adjacent mediastinal structures, and obliteration of intervening fat planes[11]. However, these have variable sensitivity and specificity[7] and are not reliable for predicting invasion. Nevertheless, preservation of fat planes indicates absence of macroscopic invasion of adjacent structures[11]. Preservation of normal sliding motion between two areas in contact is more accurate in assessing mediastinal and chest wall invasion[7]. Although both EDCT and MRI can be used, cardiac-gated MRI is superior for the aforementioned reasons.

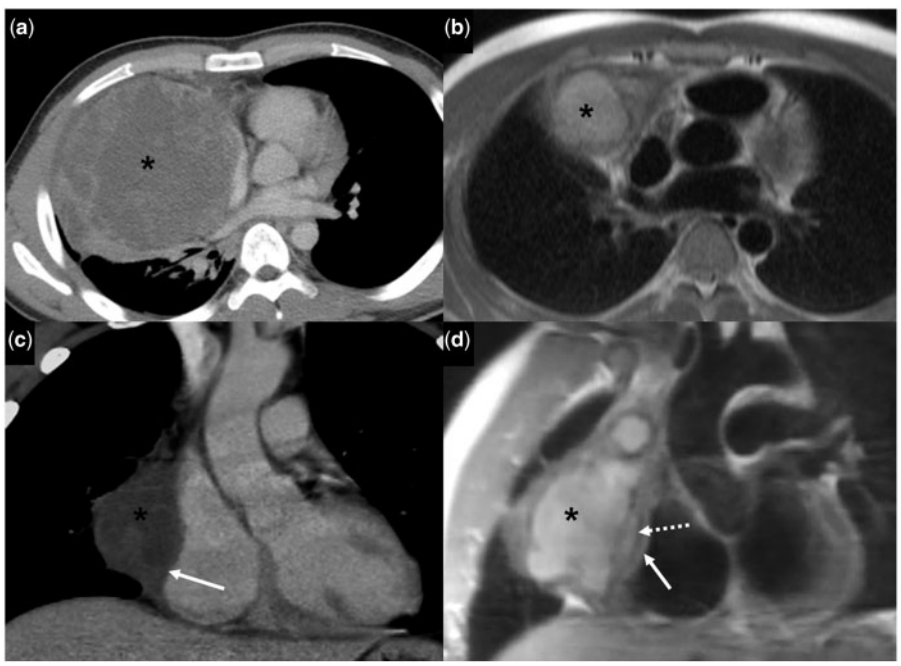

Figure 2 **A 20-year-old man with non-seminomatous germ cell tumour. (a) Initial contrast-enhanced axial CT image shows a heterogeneous mass (asterisk) with large areas of hypoattenuation in the right anterior mediastinum. (b) Follow-up axial half Fourier acquisition single short turbo spin echo (HASTE) MR image after chemotherapy shows a heterogeneously hyperintense mass (asterisk). (c) Contrast-enhanced coronal CT (after chemotherapy) shows the mass (asterisk) closely abutting the right atrium, suspicious for invasion into the pericardium and epicardial fat (solid white arrow). (d) T1W coronal oblique MR image shows that the mass (asterisk) is abutting the pericardium (dotted white arrow) overlying the right atrium. There is preservation of the epicardial fat (solid white arrow).**

Types of tumours

Thymic masses

The thymus, a lymphopoietic organ consisting of epithelial stroma and lymphocytes, arises from the third and fourth branchial pouches[12]. Its size and appearance vary with age. The gland consists predominantly of lymphoid tissue in patients below 20 years of age. It subsequently shrinks and undergoes fatty involution.

Thymic hyperplasia

There are two forms of thymic hyperplasia: true and follicular (lymphoid) hyperplasia. The thymus shows diffuse symmetrical enlargement in both. Chemical shift MRI is most sensitive for detecting microscopic fat. It helps differentiate thymic hyperplasia from tumours as thymic hyperplasia shows decreased signal intensity on opposed phase images, due to fat infiltration in normal and hyperplastic thymic tissues[13,14]. Normal histological architecture is preserved in true thymic hyperplasia[3]. The thymus may atrophy in stressful events such as chemotherapy. Post-stress, the gland grows back to its original or to a larger size, termed thymic rebound syndrome. An increased number of lymphoid follicles is seen in follicular thymic hyperplasia. This condition is seen in patients with myasthenia gravis (2/3) and autoimmune disorders, such as systemic lupus erythematosus (SLE)[12].

Thymolipoma

This is a slow-growing, benign and encapsulated tumour comprising mature adipose tissue and lymphoepithelial thymic tissue. It represents 1–10% of thymic tumours[3]. It is typically detected incidentally and is usually large with lobulated margins. On radiographs, it may mimic cardiomegaly or diaphragmatic elevation. Due to pliable consistency, they may vary in shape and location. Fatty tissue, with variable amounts of soft tissue, is seen on CT or MRI.

Thymic cyst

This represents 3% of anterior mediastinal masses[15]. They may be congenital or acquired. Acquired cysts are due to inflammation or associated with neoplasms such as seminoma. Congenital cysts are small and unilocular, whereas acquired cysts are usually larger and multilocular with walls of varying thickness. Thymic cysts are well circumscribed with contents usually of water attenuation (sometimes denser) on CT. Wall calcification may be present. On MRI, they are hypointense on T1W and hyperintense on T2W images unless there are proteinaceous or blood products.

Thymic epithelial tumours

These tumours show variable histological features and oncologic behaviour. They are classified by the World Health Organization (WHO) (updated in 2004) into two major categories: five types of thymomas (types A, AB, B1, B2, and B3) and thymic carcinomas (various histologic types including neuroendocrine carcinomas)[16]. The WHO histologic classification correlates with the clinical features and prognosis[16]. Types A and AB are usually clinically benign and encapsulated, type B has greater likelihood of invasiveness (especially type B3), and type C is almost always invasive[12].

Masaoka's surgical-pathological classification is based on surgical findings, and correlates with prognosis[3]. Tumours are classified into four stages: I, encapsulated tumour without gross or microscopic invasion of the capsule; II, macroscopic invasion into the mediastinal fat or pleura or microscopic invasion into the capsule; III, gross invasion of the adjacent organs (pericardium, great vessels and lung); IVa, pleural or pericardial spread; IVb, lymphatic or haematogenous metastases.

Thymomas have a predilection for females, with mean age of incidence in the fifth and sixth decades. Approximately 15% of myasthenic patients have thymomas, whereas 35% of patients with thymomas have myasthenia gravis. Other associations include hypogammaglobuminaemia, pure red cell aplasia and autoimmune disorders such as SLE[17].

Most old patients with thymic carcinoma are asymptomatic. Compared with thymomas, paraneoplastic manifestations are rare and prognosis is poor[3]. Thymic neuroendocrine neoplasms are rare; most frequently carcinoid tumour, which peaks in the fourth and fifth decades[17]. Paraneoplastic syndromes, mostly Cushing's syndrome, are seen in 30%. Osteoblastic metastasis is typical[3].

On CT, thymic epithelial tumours are usually homogeneous soft tissue masses. Larger lesions may have hypodense areas of old haemorrhage, necrosis or cysts. Infrequently, salt-grain calcifications are seen (Fig. 1b)[3]. On MRI, thymoma is isointense to muscle or normal thymic tissue on T1W images and heterogeneous on T2W images.

Low-risk thymomas usually have smooth contours, septation, complete or near-complete capsules and homogeneous enhancement[16]. High-risk thymomas and thymic carcinomas commonly have lobulated contours, mediastinal fat and great vessel invasion. Heterogeneous signal on T2W images are more common in invasive forms (Fig. 3)[3]. Irregular contour, necrotic or cystic components, heterogeneous enhancement, lymphadenopathy and great vessel invasion suggest thymic carcinomas[16]. Findings associated with more frequent recurrences and metastases include lobulated/irregular contours, oval shape, mediastinal fat or great vessel invasion and pleural seeding (Fig. 1a)[18].

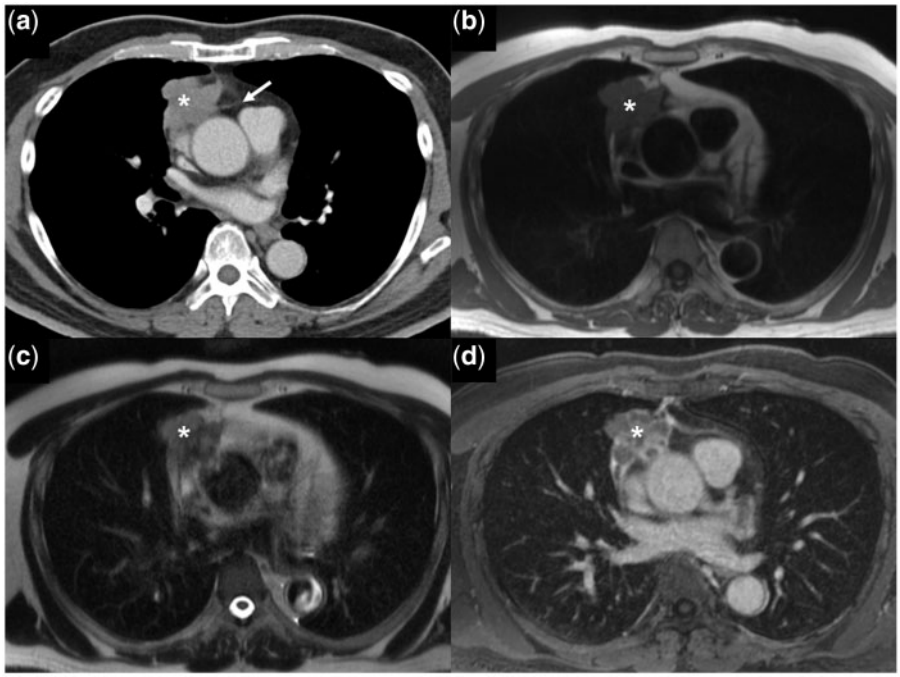

Figure 3 **A 64-year-old man with widely invasive thymoma (WHO B1). (a) Contrast-enhanced axial CT image shows an irregular mass (asterisk) in the right anterior mediastinum with infiltration of the mediastinal fat (white arrow). The mass (asterisk) is isointense on the axial T1W image (b), heterogeneously hyperintense on the T2W image (c) and shows delayed heterogeneous enhancement on the post-gadolinium T1W-fat saturated MR images (d).**

Studies show FDG-PET can differentiate thymic carcinoma from other thymic diseases but not between invasive and non-invasive thymomas[12,19]. Thymic carcinoma shows an increased standardized uptake value (SUV) compared with thymomas[12].

Germ cell tumours

Germ cell tumours (GCTs) are derived from primitive germ cells that fail to migrate completely during early embryonic development[17]. They arise along the midline between the pineal gland and presacral area, corresponding to the embryonic urogenital ridge. Mediastinal GCTs comprise up to 5% of all GCTs, and 70% of all extragonadal GCTs[3]. These are classified into teratomatous and non-teratomatous tumours[20]. Teratomatous tumours are further classified into mature teratoma, immature teratoma and teratoma with malignant transformation. The non-teratomatous tumours include seminomas and non-seminomatous tumours (endodermal sinus tumours, choriocarcinomas, embryonal carcinomas or mixed variant).

Approximately 80% of mediastinal GCTs are benign, including mature teratomas and mature teratomas containing less than 50% immature component[3]. The other subtypes are malignant. Benign GCTs are equally common in males and females, whereas malignant GCTs are predominant in males[21]. Malignant GCTs may secrete tumour markers, namely alpha-fetoprotein (α-FP) and beta-human chorionic gonadotropin (β-HCG), which aid in the diagnosis and monitoring of treatment response. Before diagnosing primary mediastinal GCTs, primary gonadal GCTs need to be excluded. The latter almost always have concomitant retroperitoneal nodal metastases[21].

Teratoma

Teratomas are common in adolescents and young adults. Mature teratomas are benign and the most common variant, accounting for 70% of mediastinal GCTs in children and 60% in adults. Histologically, they comprise irregularly arranged, well-differentiated adult tissues of ectodermal, mesodermal and endodermal origin [3]. Immature teratomas comprise the same differentiated tissues as the mature forms, together with poorly organized fetal-type tissue, mostly primitive neuroepithelial tissue. Their behaviour varies with patient age. Prognosis is good in childhood, but poor in the older age group[3].

Teratomas with malignant transformation contain a frankly malignant component, associated with fetal tissue or well-differentiated adult tissue[3]. Imaging shows laminar calcification and rarely, structured bone or teeth. On CT, they have well-defined, smooth or lobulated margins and show heterogeneous attenuation due to a combination of soft tissue, fluid, fat and calcific components (Fig. 4). Most teratomas are cystic and benign. The solid forms are usually malignant. Tumour rupture

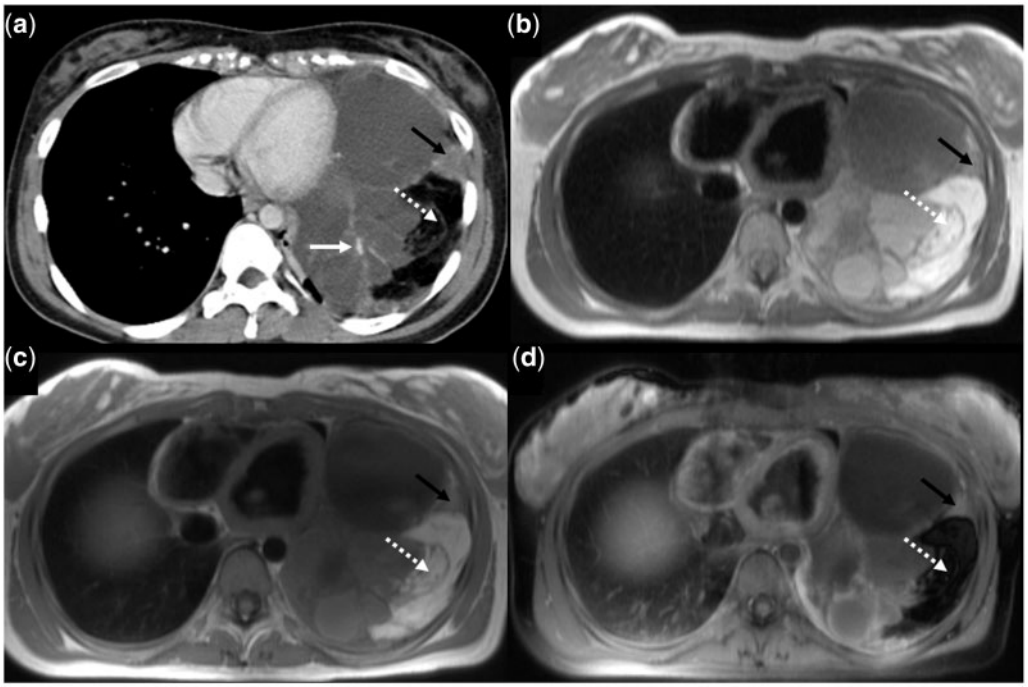

Figure 4 **A 21-year-old woman with mature teratoma. (a) Contrast-enhanced axial CT image shows a heterogeneous mass in the left lower hemithorax, containing calcification (solid white arrow), fatty component (dotted white arrow), and heterogeneous solid component (black arrow). The fatty component (dotted white arrows) is hyperintense on (b) axial HASTE and (c) T1W MR images, and hypointense on (d) post-gadolinium T1W-fat saturated MR image. Note that the calcification is difficult to see on the MR images.**

can occur secondary to local production of pancreatic enzymes. Teratomas are heterogeneous on MRI reflecting various internal elements (Fig. 4).

Seminoma

Seminoma, the second most frequent mediastinal GCT, is almost exclusive to men in the third or fourth decades. Seminomas demonstrate slow growth and metastasize later than non-seminomas. Gynaecomastia and increased oestradiol and β-HCG levels may be present[3]. Seminomas are bulky masses. On CT, they are typically solid with homogeneous density and mild enhancement. Cystic degeneration may be present. Calcification and invasion of adjacent structures are rare. Distant metastases (mostly lung, regional nodes) are possible [3]. They show intermediate signal intensity on T1W and T2W images.

Non-seminomatous GCTs

About 85% of non-seminomatous GCTs occur in men with a mean age of 29 years. These are associated with Klinefelter's syndrome (in 20%)[3], and haematological and solid cancers. Patients usually have increased lactate dehydrogenase (LDH), α-FP and β-HCG levels[3]. Radiologically, a bulky irregular mass is seen, with heterogeneous density on CT due to central hypodense areas of necrosis, haemorrhage and cystic degeneration (Fig. 2a)[3]. There may be invasion of adjacent structures, locoregional nodal metastases and distant metastases. Pleural and pericardial effusions are common. On MRI, the tumours show heterogeneous signal intensity with areas of hyperintensity reflecting degenerative cystic changes on T2W images(Fig. 2b).

Lymphoma

Lymphoma may present as a primary mediastinal lesion or, more commonly, as a systemic disease. Many primary mediastinal lymphomas arise in the thymus rather than lymph nodes[3]. In adults, Hodgkin lymphoma (HL) of the nodular sclerosing type is most frequent; whereas in children, non-Hodgkin lymphoma (NHL) predominates. The most common variants of NHL are diffuse large B-cell lymphoma and T-cell lymphoblastic lymphoma. Tateishi et al.[22] described CT findings that differentiate these three most common subtypes. Characteristic features of HL are irregular contour of the anterior mediastinal mass, surface lobulation, absence of vascular involvement, pleural effusion and associated mediastinal lymphadenopathy. Features of diffuse large B-cell lymphoma are regular contour, presence of vascular involvement and absence of cervical and abdominal lymphadenopathy. Features of T-cell lymphoblastic lymphoma are regular contour, presence of pericardial

effusion and associated cervical and abdominal lymphadenopathy and splenomegaly[22].

Differentiating treated bulky lesions from residual tumour is difficult, especially on CT. Both residual and sterilized tumours are heterogeneous on T2W images[21]. A hyperintense signal on T2W images and a hypointense signal on T1W images may represent residual active lymphoma, immature fibrotic tissue, areas of necrosis or inflammation[21,23]. Sterilized tumours are heterogeneous on T2W and T1W images due to mixed fat and fibrous tissue. Inactive residual fibrotic masses are homogeneously hypointense. Gadolinium-enhanced MRI is useful as enhancement decreases markedly after treatment in patients in complete remission but not in patients with relapse[21].

Gallium-67 (^{67}Ga) scintigraphy and FDG-PET are useful in disease staging and follow-up after treatment. However, FDG-PET is superior to ^{67}Ga scintigraphy regarding specificity for and detection of malignant lymphoma, except for indolent lymphoma[24]. Residual lesions with positive PET findings suggest aggressive lymphoma, but negative PET findings do not necessarily indicate that the patient is disease free[24]. Persistent FDG uptake after chemotherapy is associated with poor clinical outcome[25].

Hodgkin lymphoma

HL has a bimodal age distribution in young adulthood and after the fifth decade[17]. Patients may present with systemic symptoms (category B); SVC syndrome and infiltration of the chest wall are rare[3]. Most patients present with disease located above the diaphragm (stage I–II according to the Ann Arbor classification), and fewer than 10% have extranodal disease at presentation (stage IV)[3]. Chest radiography is usually abnormal. Spread occurs via contiguous nodal stations, most frequently anterior mediastinal and paratracheal nodes. Pulmonary invasion is associated with hilar nodal involvement. On CT, the mass may consist of multiple enlarged nodes, a bulky mass (nodal conglomerates) or a solid thymic lesion (less commonly cystic). There may be displacement, compression or invasion of mediastinal structures. The density is often homogeneous, but larger lesions may be heterogeneous. Calcification is typically present after treatment. On MRI, the mass is fairly homogeneous, isointense to muscle on T1W images and isointense to fat on T2W images.

Non-Hodgkin lymphoma

Patients usually present with advanced disease, systemic symptoms (category B), generalized lymphadenopathy or extranodal disease. Histopathological classification has greater prognostic significance than anatomical extension of disease[3].

Large B-cell lymphoma is seen in young adults and occasionally children, with a prevalence in females. Presentation is subacute and occasionally has features of an oncological emergency (mediastinal syndrome) due to rapid growth of the mass which may infiltrate the SVC, airways or other adjacent structures[3]. On CT, the tumours show hypodense areas of haemorrhage, necrosis, or cystic degeneration and heterogeneous enhancement. On MRI, the solid component is slightly hyperintense to muscle on T1W and hyperintense on T2W images (Fig. 5). The tumours are large, commonly invading the adjacent mediastinal structures, chest wall, and lung. Pleural and pericardial effusions are seen in 1/3.

Lymphoblastic lymphomas are aggressive tumours, occurring in the first two decades, more often in males. On CT, a large mediastinal mass, with necrotic areas, compressing the airway and cardiovascular structures is seen. Pleural and pericardial effusions are frequent. There is a predilection for rapid dissemination and extensive involvement, including extrathoracic nodes, bone marrow, central nervous system and gonads[21].

Thyroid mass

Substernal goitre represents 10% of mediastinal masses[26], and is usually a benign multinodular colloid goitre or adenoma, rarely a carcinoma. Approximately 3/4 extend into the anterior mediastinum and 1/4, the posterior mediastinum[26]. On CT, this is continuous with the cervical thyroid gland[26,27] and may cause tracheal deviation. Calcific foci are common. Goitre shows attenuation greater than 100 Hounsfield Units (HU) on pre-contrast CT, and avid prolonged enhancement post-contrast. Hypodense areas representing haemorrhage and cysts may be present.

Distinguishing between benign and malignant goitres is impossible unless the tumour invades beyond the thyroid gland[27,28]. Associated lymphadenopathy and extension into the mediastinal fat or chest wall suggest malignancy (Fig. 6). MRI is highly accurate in detecting invasion of adjacent structures[29]. Effacement of fat in the tracheoesophageal groove or between the laryngeal cartilage and hypopharyngeal wall predicts recurrent laryngeal nerve invasion[29].

Scintigraphy with iodine-123 (^{123}I) detects ectopic thyroid tissue[30]. After thyroidectomy for differentiated thyroid cancer, ^{131}I scintigraphy helps detect remnant thyroid tissue and functioning metastases[30].

Parathyroid masses

Ectopic parathyroid glands may occur in or near the thymus, or aorto-pulmonary window. At CT, an ectopic parathyroid may simulate a lymph node. Scintigraphy is more effective in their detection than CT or MRI. Parathyroid scintigraphy is extremely sensitive (90%) for localizing parathyroid adenomas but is only 60% sensitive for detecting hyperplasia[31]. The sensitivity and

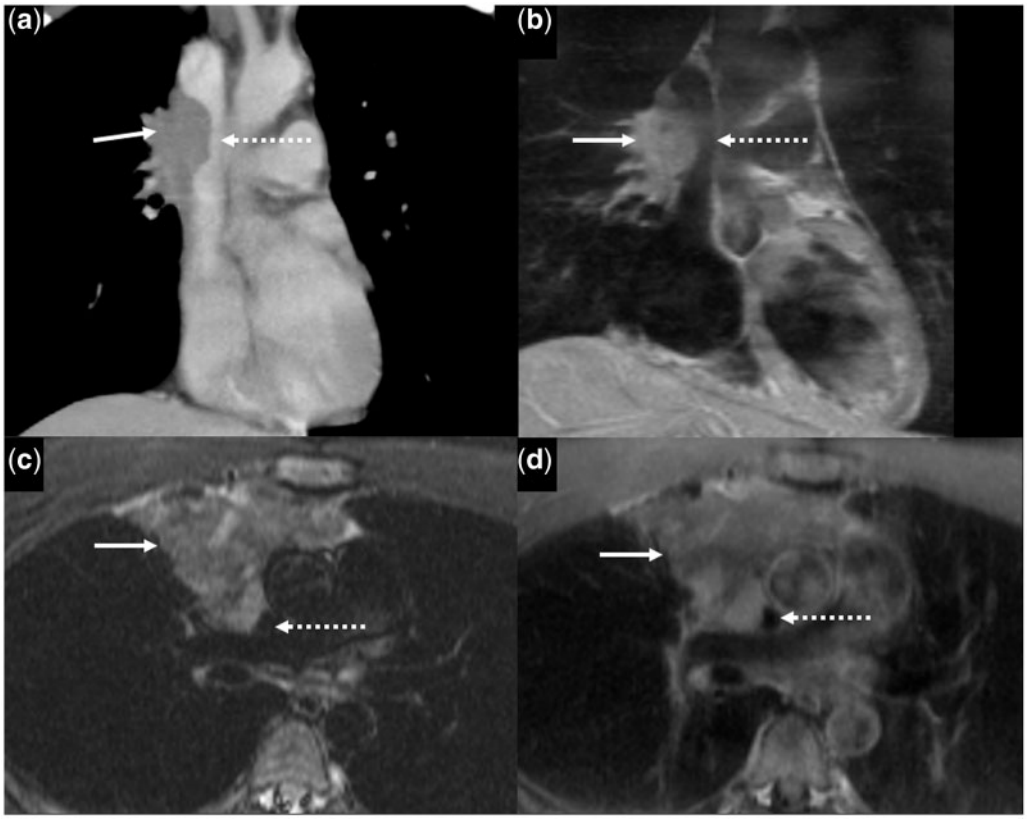

Figure 5 **A 22-year-old man with diffuse large B-cell lymphoma; presented with symptoms of SVC obstruction. (a) Contrast-enhanced coronal CT image shows an irregular mass (solid white arrow) causing narrowing of the SVC (dotted white arrow). (b) Corresponding coronal post-gadolinium T1W-fat saturated MR image shows the same findings. The mass is hyperintense on (c) short tau inversion recovery (STIR) MR image and shows heterogeneous enhancement on (d) post-gadolinium T1W-fat saturated MR image.**

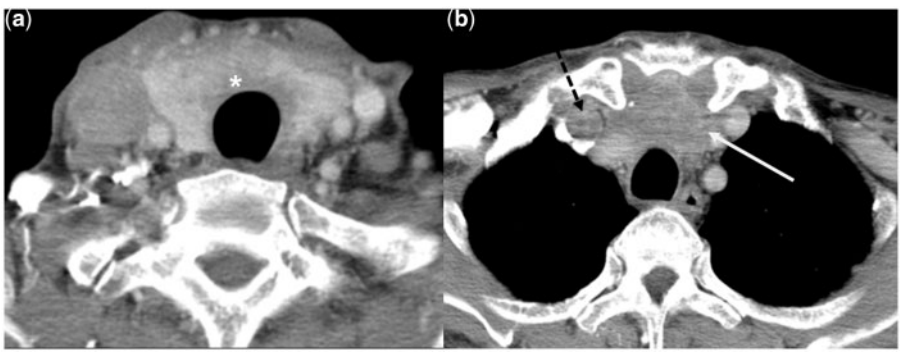

Figure 6 **A 70-year-old man with undifferentiated carcinoma of the thyroid. Contrast-enhanced axial CT images show an ill-defined heterogeneously enhancing mass (asterisk) arising from the thyroid gland, and extending to the superior mediastinum (white arrow). There is a filling defect in the right internal jugular vein in keeping with thrombosis (dotted black arrow in b).**

specificity is affected by the size and cellularity of the glands and the parathyroid hormone level. Small or weakly avid glands may not be detected at scintigraphy[31].

Mesenchymal masses

Mesenchymal masses account for 5% of all mediastinal masses. They arise from mesenchymal elements, namely fat, fibrous tissue, smooth and striated muscle, blood and

Figure 7 **A 63-year-old woman with mediastinal liposarcoma. Contrast-enhanced axial CT image shows a mass with soft tissue (dotted white arrows) and fatty component (dotted black arrow) in the anterior mediastinum. Adjacent atelectasis is seen in the left lung (solid black arrow). Bilateral breast implants (asterisk) are present.**

lymphatic vessels, bone and nerve tissue. Half of the mesenchymal masses are malignant[3].

Lipoma

Extrathymic lipoma is the most common non-neurogenic mesenchymal tumour of the mediastinum and accounts for 2% of all mediastinal masses[3]. Lipomas are typically asymptomatic and can reach remarkable dimensions. At chest radiography, they appear as poorly radiopaque bulky multi-lobulated masses. They change their shape according to the patient's position.

Liposarcomas

Liposarcomas are extremely rare and occur in the fifth decade[3]. They may originate in the thymus, but the most frequent site is the posterior mediastinum[3]. Most patients present with locally advanced disease with signs and symptoms of compression. Radiologically, the disease presents as a bulky, well-marginated mediastinal mass. The well-differentiated forms show areas of fat density associated with areas of soft tissue density (Fig. 7), whereas the poorly differentiated forms show homogeneous soft tissue density[3]. Extrathoracic metastasis is rare.

Lymphangioma

Lymphangioma is a benign rare congenital malformation of the lymphatic vessels. It is usually seen in the cervical region but can extend into the mediastinum in 10% of cases, which may be associated with chylothorax and haemangiomas[17].These tumours are lobulated and multi-cystic, and can reach a massive size. They may surround or displace mediastinal structures and may infiltrate across tissue planes. On CT, they are usually near water attenuation, with septa that may enhance minimally after contrast administration.

Haemangioma

Haemangiomas account for 0.5% of all mediastinal tumours and represent the most common vascular tumour in the mediastinum[3]. They may occur anywhere in the body, of which 60% are seen in the anterior mediastinum and 25% in the posterior compartment[3]. They are heterogeneous masses on CT/MRI, with phleboliths seen in 30%.

Conclusion

Anterior mediastinal masses comprise a wide spectrum of tumours. Multimodality imaging is important in characterizing and staging of these tumours. Although conventional CT remains the modality of choice, cardiac-gated MRI has an increasingly important role, especially in tissue characterization and assessment of surgical resectability.

References

[1] Davis RD, Jr. Oldham HN Jr, Sabiston DC. Jr. Primary cysts and neoplasms of the mediastinum: recent changes in clinical presentation, methods of diagnosis, management, and results. Ann Thorac Surg 1987; 44: 229–237. doi:10.1016/S0003-4975(10)62059-0. PMid:2820323.

[2] Cameron RB, Loehrer PJ, Thomas CR. Neoplasms of the mediastinum. In: DeVita VT, Lawrence TS, Rosenberg SA, editors. DeVita, Hellman, and Rosenberg's cancer: principles & practice of oncology. Vol. 1. 8th ed. Philadelphia, PA: Lippincott Williams & Wilkins; 2008, p. 973.

[3] Priola AM, Priola SM, Cardinale L, Cataldi A, Fava C. The anterior mediastinum: diseases. Radiol Med 2006; 111: 312–342. doi:10.1007/s11547-006-0032-5. PMid:16683081.

[4] Priola SM, Priola AM, Cardinale L, Perotto F, Fava C. The anterior mediastinum: anatomy and imaging procedures. Radiol Med 2006; 111: 295–311. doi:10.1007/s11547-006-0031-6. PMid:16683080.

[5] Whitten CR, Khan S, Munneke GJ, Grubnic S. A diagnostic approach to mediastinal abnormalities. Radiographics 2007; 27: 657–671. doi:10.1148/rg.273065136. PMid:17495284.

[6] Murata K, Takahashi M, Mori M, et al. Chest wall and mediastinal invasion by lung cancer: evaluation with multisection expiratory dynamic CT. Radiology 1994; 191: 251–255. PMid:8134583.

[7] Seo JS, Kim YJ, Choi BW, Choe KO. Usefulness of magnetic resonance imaging for evaluation of cardiovascular invasion: evaluation of sliding motion between thoracic mass and adjacent structures on cine MR images. J Magn Reson Imaging 2005; 22: 234–241. doi:10.1002/jmri.20378. PMid:16028243.

[8] Akata S, Kajiwara N, Park J, et al. Evaluation of chest wall invasion by lung cancer using respiratory dynamic MRI. J Med Imaging Radiat Oncol 2008; 52: 36–39. doi:10.1111/j.1440-1673.2007.01908.x. PMid:18373824.

[9] Kodalli N, Erzen C, Yüksel M. Evaluation of parietal pleural invasion of lung cancers with breathhold inspiration and expiration MRI. Clin Imaging 1999; 23: 227–235. doi:10.1016/S0899-7071(99)00135-7. PMid:10631899.

[10] Bacha EA, Chapelier AR, Macchiarini P, Fadel E, Dartevelle PG. Surgery for invasive primary mediastinal tumors. Ann Thorac

Surg 1998; 66: 234–239. doi:10.1016/S0003-4975(98)00350-6. PMid:9692471.

[11] Shaham D, Skilakaki MG, Goitein O. Imaging of the mediastinum: applications for thoracic surgery. Thorac Surg Clin 2004; 14: 25–42. doi:10.1016/S1547-4127(04)00039-8. PMid: 15382306.

[12] Nishino M, Ashiku SK, Kocher ON, Thurer RL, Boiselle PM, Hatabu H. The thymus: a comprehensive review. Radiographics 2006; 26: 335–348. doi:10.1148/rg.262045213. PMid:16549602.

[13] Inaoka T, Takahashi K, Mineta M, et al. Thymic hyperplasia and thymus gland tumors: differentiation with chemical shift MR imaging. Radiology 2007; 243: 869–876. doi:10.1148/radiol.2433060797. PMid:17463136.

[14] Takahashi K, Inaoka T, Murakami N, et al. Characterization of the normal and hyperplastic thymus on chemical-shift MR imaging. AJR Am J Roentgenol 2003; 180: 1265–1269. PMid: 12704035.

[15] Bogot NR, Quint LE. Imaging of thymic disorders. Cancer Imaging 2005; 5: 139–149. doi:10.1102/1470-7330.2005.0107. PMid:16361143.

[16] Sadohara J, Fujimoto K, Müller NL. Thymic epithelial tumors: comparison of CT and MR imaging findings of low-risk thymomas, high-risk thymomas, and thymic carcinomas. Eur J Radiol 2006; 60: 70–79. doi:10.1016/j.ejrad.2006.05.003. PMid: 16766154.

[17] Duwe BV, Sterman DH, Musani AI. Tumors of the mediastinum. Chest 2005; 128: 2893–2909. doi:10.1378/chest.128.4.2893. PMid:16236967.

[18] Jeong YJ, Lee KS, Kim J, et al. Does CT of thymic epithelial tumors enable us to differentiate histologic subtypes and predict prognosis? AJR Am J Roentgenol 2004; 183: 283–289. PMid:15269013.

[19] Ferdinand B, Gupta P, Kramer EL. Spectrum of thymic uptake at 18F-FDG PET. Radiographics 2004; 24: 1611–1616. doi:10.1148/rg.246045701. PMid:15537971.

[20] Moran CA, Suster S. Primary germ cell tumors of the mediastinum: I. Analysis of 322 cases with special emphasis on teratomatous lesions and a proposal for histopathologic classification and clinical staging. Cancer 1997; 80: 681–690. doi:10.1002/(SICI)1097-0142(19970815)80:4<681::AID-CNCR6>3.0.CO;2-Q. PMid:9264351.

[21] Takahashi K, Al-Janabi NJ. Computed tomography and magnetic resonance imaging of mediastinal tumors. J Magn Reson Imaging 2010; 32: 1325–1339. doi:10.1002/jmri.22377. PMid:21105138.

[22] Tateishi U, Müller NL, Johkoh T, et al. Primary mediastinal lymphoma: characteristic features of the various histological subtypes on CT. J Comput Assist Tomogr 2004; 28: 782–789. doi:10.1097/00004728-200411000-00009. PMid:15538151.

[23] Rahmouni A, Luciani A, Itti E. MRI and PET in monitoring response in lymphoma. Cancer Imaging 2005; 5(A): S106–112.

[24] Okada M, Sato N, Ishii K, Matsumura K, Hosono M, Murakami T. FDG PET/CT versus CT, MR imaging, and ^{67}Ga scintigraphy in the posttherapy evaluation of malignant lymphoma. Radiographics 2010; 30: 939–957. doi:10.1148/rg.304095150. PMid:20631361.

[25] Cronin CG, Swords R, Truong MT, et al. Clinical utility of PET/CT in lymphoma. AJR Am J Roentgenol 2010; 194: W91–103. doi:10.2214/AJR.09.2637. PMid:20028897.

[26] Tecce PM, Fishman EK, Kuhlman JE. CT evaluation of the anterior mediastinum: spectrum of disease. Radiographics 1994; 14: 973–990. PMid:7991827.

[27] Quint LE. Imaging of anterior mediastinal masses. Cancer Imaging 2007; 7(A): S56–62.

[28] Laurent F, Latrabe V, Lecesne R, et al. Mediastinal masses: diagnostic approach. Eur Radiol 1998; 8: 1148–1159. doi:10.1007/s003300050525. PMid:9724429.

[29] Kabala JE. Computed tomography and magnetic resonance imaging in diseases of the thyroid and parathyroid. Eur J Radiol 2008; 66: 480–492. doi:10.1016/j.ejrad.2008.03.030. PMid: 18502599.

[30] Intenzo CM, Dam HQ, Manzone TA, Kim SM. Imaging of the thyroid in benign and malignant disease. Semin Nucl Med 2012; 42: 49–61. PMid:22117813.

[31] Smith JR, Oates ME. Radionuclide imaging of the parathyroid glands: patterns, pearls, and pitfalls. Radiographics 2004; 24: 1101–1115. doi:10.1148/rg.244035718. PMid:15256632.